

Electronic structure of $\text{LaFeAsO}_{1-x}\text{F}_x$ from x-ray absorption spectroscopy

T. Kroll,^{1,*} S. Bonhommeau,² T. Kachel,² H. A. Dürr,² J. Werner,¹ G. Behr,¹ A. Koitzsch,¹ R. Hübel,¹ S. Leger,¹ R. Schönfelder,¹ A. K. Ariffin,³ R. Manzke,³ F. M. F. de Groot,⁴ J. Fink,^{1,2} H. Eschrig,¹ B. Büchner,¹ and M. Knupfer¹

¹IFW Dresden, P.O. Box 270116, D-01171 Dresden, Germany

²BESSY, Albert-Einstein-Strasse 15, 12489 Berlin, Germany

³Institut für Physik, Humboldt-Universität zu Berlin, Newtonstrasse 15, 12489 Berlin, Germany

⁴Department of Inorganic Chemistry and Catalysis, Utrecht University, Sorbonnelaan 16, 3584 CA Utrecht, The Netherlands

(Received 20 June 2008; revised manuscript received 24 October 2008; published 3 December 2008)

We investigated the recently found superconductor $\text{LaFeAsO}_{1-x}\text{F}_x$ by x-ray absorption spectroscopy. From a comparison of the O K edge with LDA calculations we find good agreement and are able to explain the structure and changes in the spectra with electron doping. From experimental Fe $L_{2,3}$ -edge spectra and charge-transfer multiplet calculations we gain further information on important physical values such as the hopping parameters, the charge-transfer energy Δ , and the Hubbard U . Furthermore we find the system to be very covalent with a large amount of ligand holes. A shift in the chemical potential is visible in the O K - and Fe $L_{2,3}$ -edge spectra which emphasizes the importance of band effects in these compounds. From the entirety of our results we conclude that LaFeAsO is a bandwidth-dominated material.

DOI: 10.1103/PhysRevB.78.220502

PACS number(s): 71.20.-b, 71.70.Ch, 78.70.Dm

Recent reports of superconductivity in $\text{LaFeAsO}_{1-x}\text{F}_x$ (Refs. 1 and 2) stimulated enormous scientific efforts. In fact, a large oxypnictides family $\text{LnFeAsO}_{1-x}\text{F}_x$ ($\text{Ln}=\text{La}, \text{Ce}, \text{Pr}, \text{Nd}, \text{Sm}, \text{and Gd}$) has been found to be superconducting with a transition temperature up to 55 K (Refs. 3–5) and high upper critical fields.⁶ These compounds are particularly interesting as they are an example of possible unconventional superconductivity with a large transition temperature in a noncuprate transition-metal compound. Their crystal structure is similar to high- T_c cuprates. Both have a layered structure in which the role of the CuO_2 planes is now played by FeAs, mediated by (doped) LnO layers that behave as charge reservoirs.

In order to gain a better understanding of these compounds, various experiments and theoretical calculations have been carried out. Possible unconventional multiband behavior^{7,8} and evidence for gap nodes^{9,10} have been considered from experiments and theoretical studies, while various scenarios for the superconducting mechanism have been discussed.^{11–13} Nuclear-magnetic-resonance (NMR) measurements find evidence for line nodes in the superconducting gap and spin-singlet pairing in the superconducting state,¹⁴ while Andreev spectroscopy finds a single nodeless BCS-type gap.¹⁵ Electronic structure calculations within the local-density approximation (LDA) show a high density of Fe $3d$ states near the Fermi level, whereas the density of states (DOS) for all other ions is low.^{7,8,12,13,16} LDA plus dynamical-mean-field theory (DMFT) as well as LDA calculations that include Hubbard's U conclude an intermediate strength of $U \sim 1\text{--}4$ eV and Hund's exchange coupling $J_H \sim 0.3\text{--}0.9$ eV at the Fe site,^{7,17–21} and the undoped system has been predicted to exhibit a bad metallic behavior.^{17,22}

Core-level spectroscopic measurements such as x-ray absorption spectroscopy (XAS) are appropriate experimental methods to shed light on this topic. In XAS, a core electron is excited into an unoccupied state near the Fermi level, i.e., one probes the empty states. Combined with a theoretical description that takes the core hole and other contributions properly into account, it can provide valuable information on

the electronic structure of the investigated system, such as the Hubbard U , the charge-transfer energy Δ , the Hund coupling J , or the electronic hopping parameters. In this Rapid Communication, we present experimental data from O K - and Fe $L_{2,3}$ -absorption edges. For these measurements we chose undoped LaFeAsO and electron-doped $\text{LaFeAsO}_{1-x}\text{F}_x$ polycrystalline samples in a doping range between $x=0.0$ and 0.15. These data will be discussed and compared to LDA calculations as well as to Fe $3d$ charge-transfer multiplet calculations.

Polycrystalline samples of $\text{LaFeAsO}_{1-x}\text{F}_x$ were prepared as pellets as described in Ref. 23. The samples have been characterized by x-ray diffraction, magnetization, transport, and local probes such as muon spin relaxation (μSR) and NMR measurements. Critical temperatures for $x=0.075, 0.1,$ and 0.15 have been found at $T_c=22, 26.8,$ and 9.9 K, respectively.^{14,24}

X-ray absorption spectroscopy studies at the O K and Fe $L_{2,3}$ edges were performed at the PM3 beamline of the synchrotron-radiation source Bessy II. The energy resolutions were set to 180 and 300 meV at 530 and 710 eV photon energies, respectively. Data were recorded by measuring the fluorescence signal. In order to obtain appropriate surfaces, the pellets were filed *in situ* in a vacuum environment of 1×10^{-7} mbar and measured at 1×10^{-8} mbar.

In Fig. 1(a) O K -edge spectra are shown for photon energies between 529 and 539 eV. This region can be assigned to excitations from the O $1s$ core level into unoccupied O $2p$ states. In the XAS spectra the onset of peak (1) shifts by 0.35 eV toward higher photon energies with doping,²⁵ whereas peak (1) itself shifts only by ≈ 100 meV and peak (2) [and also peak (4)] does not shift.

The oxygen p -projected density of states (p -PDOS) as gained from LDA calculations⁸ is shown in Figs. 1(b) and 1(c) for $x=0.0$ and $x=0.125$. The PDOS has been broadened by a Gaussian with full width at half maximum (FWHM) of 0.18 eV and a Lorentzian with FWHM of 0.2 eV. From the LDA PDOS, peak (1) can be ascribed to a hybridization of O states with Fe $3d$ states and peak (2) to hybridization with

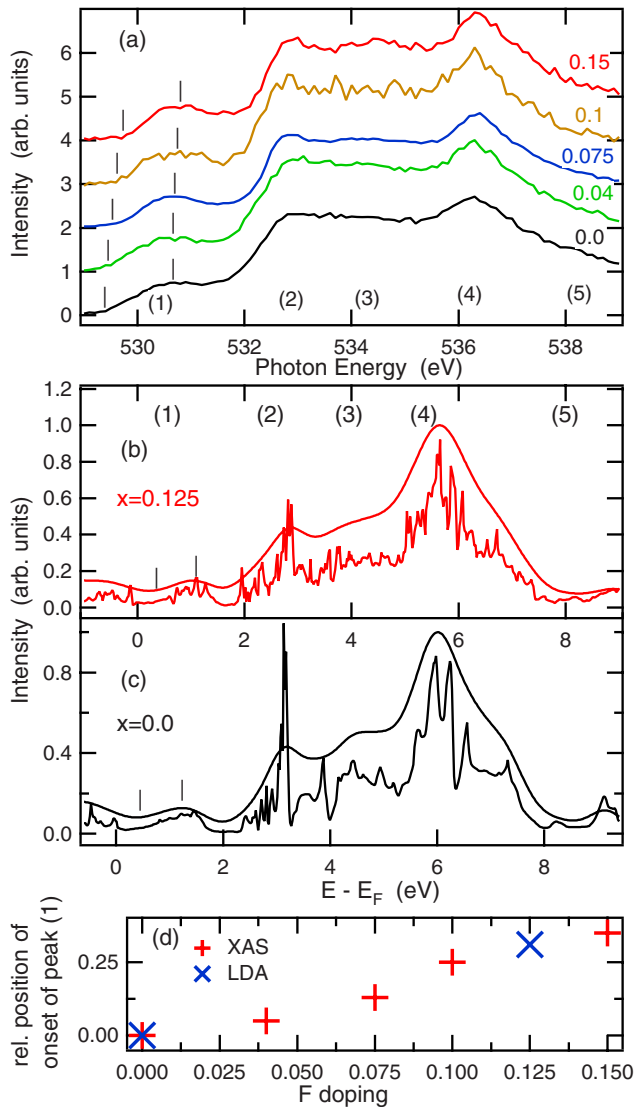


FIG. 1. (Color online) LaFeAsO_{1-x}F_x: (a) doping dependence of XAS O K-edge spectra. The spectra have been normalized at 610 eV where they become structureless. (b), (c) Oxygen *p*-projected partial density of states for $x=0.0$ and $x=0.125$. (d) Energy shift of the onset of peak (1) as compared to $x=0.0$ for experimental and theoretical results.

La *4f* states. The position of peak (1) essentially measures the Madelung potential at the Fe layers, while the position of peak (2) is related to the Madelung potential at the La layer. One effect of doping is a change in the Madelung potentials. According to LDA, the Madelung potential for La sites should hardly change as compared to the O site, whereas for Fe it leads to a shift of peak (1) toward higher energies, which is corroborated by the XAS data at the O *K* edge and photoemission spectroscopy.²⁶ A second and more important effect with electron doping is a shift of the chemical potential due to a change in the carrier number. By this, the onset of peak (1) is further shifted to higher energies as compared to the La peak.

When comparing the experimental and theoretical results, one observes, first of all, that the overall agreement is good, which tells us that apparently the core hole effect in the

absorption process is small. Therefore a direct interpretation of XAS measurements in terms of the partial unoccupied density of states is possible, analogous to one-electron addition process.²⁷ Note that the energies as given in Figs. 1(a)–1(c) correspond to different reference values. In XAS the photon energy relates to the energy difference between the core level and the unoccupied states, whereas in the PDOS the energy difference between the Fermi level and the unoccupied states is given. For the sake of clarity the energy regions in Figs. 1(b) and 1(c) are chosen in such a way that peak (2) aligns with the experimental data. When focusing on the onset of peak (1), i.e., on the change in the chemical potential, a clear doping dependence is observed. This is illustrated in Fig. 1(d) where the shift of the onset of peak (1) as compared to $x=0.0$ is shown. Such an increase is supported by the PDOS since the shift in the onset of peak (1) (Ref. 25) between $x=0.0$ and $x=0.125$ matches well to the slope found from the experimental data. This agreement between theory and experiment stresses the observation that the experimental O *K* edge is strongly affected by the shift of the chemical potential with doping.

Furthermore, in LDA no Coulomb energy U is taken into account. When switching it on at the Fe site, this will have an effect on the energetic position of the Fe *3d* spectral weight. As the relative position of the O *K* XAS peaks matches those determined by LDA calculations within 1 eV, together with the observation that the LaFeAsO valence-band spectrum can be explained by the DOS as derived from LDA (Ref. 26) but does not match the DOS as derived from LDA+ U (Ref. 7) or DMFT,¹⁷ we conclude that U is small as compared to the conduction-band width.

In order to gain more information on the electronic structure, XAS experiments at the Fe *L*_{2,3} edge have been performed. According to the dipole selection rules, the Fe *L*_{2,3} absorption edges correspond to excitations of Fe *2p* core-level electrons into unoccupied Fe *3d* electronic states. Contrary to what occurs at the O *K* edge, core holes cannot be neglected for Fe *3d* excitations. Therefore, simulations of the Fe *L*_{2,3} edge require consideration of multiplet splitting, hybridization, and crystal-field effects. Fe *L*_{2,3}-edge experimental data have been taken by recording the fluorescence yield and corrected for a self-absorption process.²⁸ Self-absorption is stronger at the *L*₃ edge, which cannot be fully corrected, and thereby the *L*₃-edge intensity will be somewhat underestimated as compared to the *L*₂ edge. All data have been normalized at 750 eV where the signal corresponds to excitations into continuum states.

In Figs. 2(a) and 2(b) the experimental Fe *L*₃-edge XAS spectra for different doping levels are shown. Two main changes appear with F doping. The energy position of the main peak around 708 eV shifts slightly with doping toward lower energies. This shift amounts to ≈ 150 meV on going from $x=0.0$ to $x=0.15$ and can be explained by the observation that the x-ray photoemission spectroscopy (XPS) Fe *2p* core-level excitations do not shift relative to the chemical potential with doping within the experimental resolution,²⁹ while the chemical potential shifts by ≈ 200 meV with doping from $x=0.0$ and $x=0.2$.²⁶ In other words, this excitation energy as seen in Fig. 2 decreases upon doping. Moreover, the onset of the *L*₃ edge²⁵ shifts to higher photon energies by

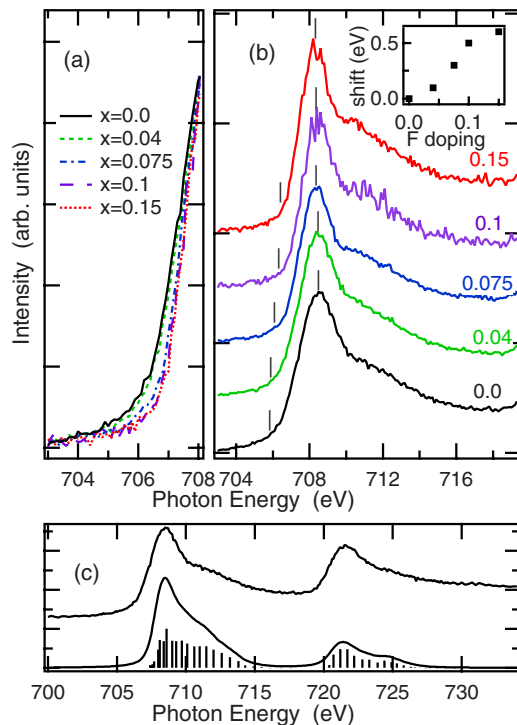


FIG. 2. (Color online) $\text{LaFeAsO}_{1-x}\text{F}_x$: doping dependence of the Fe $L_{2,3}$ edge. (a) Blowup of the low-energy side of experimental Fe L_3 edge. For the sake of clarity, the spectra in (a) were shifted in such a way that their maxima match. (b) Experimental L_3 edge for the same doping range. The inset shows the shift of the onset of the main peak in eV relative to $x=0.0$ as a function of doping x . (c) Comparison of LaFeAsO XAS spectrum with charge-transfer multiplet calculation (for values see text).

≈ 600 meV, similar to the O K edge. Such a shift could also cause an asymmetric peak narrowing and affect the position of the peak maxima. In Fig. 2(a) a blowup of the low-energy side of the L_3 peak is shown. Note that for the sake of clarity, the spectra only in Fig. 2(a) were shifted to the same energy of their maxima. A shifted onset is consistent with additional electrons at the Fe sites which diminishes the number of holes, i.e., the total intensity at the Fe L edge. Therefore, the doped electrons reside (partially) on the Fe sites. These findings are supported by valence-band photoemission spectroscopy.²⁶ Since the conduction band is partially filled, this shift leads to the experimentally observed effect on the Fe $L_{2,3}$ edge and emphasizes the importance of band effects on the absorption edge in these compounds. Similar to what has been observed at the O K edge, the onset of the spectra shifts monotonically to higher energies [see the inset of Fig. 2(b)] and stresses the shift of the chemical potential as the origin of both effects.

Although As is formally As^{3-} , its $4p$ shell is not completely filled due to hybridization with the Fe $3d$ shell. The radial function of $4p$ states is far ranging compared to the $2p$ states of O as in copper oxides. Therefore, a large overlap of the wave functions between Fe and As occurs which leads to a strong hybridization and a further delocalization of the Fe $3d$ electrons. With F doping delocalized additional charge is introduced into this layer. When looking at the crystal

structure, the FeAs layers consist of Fe ions on a square lattice that are tetrahedrally surrounded by four As ions. These As tetrahedra are slightly tetragonally distorted. The crystal-field splitting $10Dq$ has been predicted to be rather small (~ 0.25 eV).^{7,18} From LDA plus DMFT calculations the $d_{x^2-y^2}$ and $d_{3z^2-r^2}$ orbitals have been found to be still degenerate²² and the E_g/T_{2g} splitting to be dominant over the tetragonal distortion. Therefore, it is reasonable to use T_d local symmetry as a starting point for simulations of the Fe L edge. In an x-ray absorption excited state, a $2p$ core hole has been created which interacts with valence electrons via Coulomb interactions. This interaction justifies a local description also of a metallic system as long as it is strong enough to lift the excited states out of the conduction band.

In order to interpret the experimental data further, we performed charge-transfer multiplet calculations for divalent Fe^{2+} ($3d^6$).³⁰⁻³³ The calculations have been done for T_d symmetry and the hopping relation $V_e = \frac{1}{\sqrt{3}}V_{t_2}$, assuming the relation $pd\sigma = -\frac{\sqrt{3}}{4}pd\pi$. Note that a band effect such as the shift of the chemical potential is beyond this local approach. In Fig. 2(c) a comparison of the XAS fluorescence data and charge-transfer multiplet calculation is shown. The agreement between experiment and theory at the $L_{2,3}$ edge is good. Note that the intensity of the L_2 edge is overestimated by the self-absorption correction. The parameter set that best reproduces the experimental data is $10Dq=0.2$ eV, $\Delta = d^7\bar{L} - d^6 = 1.25$ eV (\bar{L} denotes a ligand hole), $U=1.5$ eV (multiplet averaged), and $|pd\pi|=0.27$ eV. The core hole potential Q is normally about 1–2 eV larger than U and has been set to $Q=U+1$ eV. The Slater-Condon parameters have been reduced to 80% of their Hartree-Fock values as it is reasonable in solids, which leads to the two Hund couplings $J_{e_g}=0.90$ eV and $J_{t_{2g}}=0.78$ eV for the ground state. The shoulder at ≈ 712 eV is provoked by charge-transfer effects and emphasizes the hopping values above. A square band containing five states and a bandwidth of 2.5 eV for the ligand hole state has been added in the charge-transfer calculations. The multiplet intensities have been broadened by a Gaussian (0.3 eV) and a Lorentzian (0.6 eV at L_3 and 0.8 eV at L_2 due to different lifetime broadenings). Since the core hole potential is rather small (≈ 2.5 eV), the excited states are not shifted far out of the Fe $3d$ band at ≈ 2 eV above the Fermi energy, and therefore band effects become visible. When writing the wave function as a sum of three configurations with different ligand holes $|\psi\rangle = a|d^6\rangle + b|d^7\bar{L}^1\rangle + c|d^8\bar{L}^2\rangle$ ($a^2 + b^2 + c^2 = 1$), the hole occupation can be given. Using the above parameters, it follows that $a^2=0.558$, $b^2=0.393$, and $c^2=0.049$. For all possible parameter sets, a high spin situation $S=2$ has been determined in agreement with LDA+DMFT.²² The energy difference to the intermediate spin state $S=1$ is ≈ 0.4 eV which is enough to omit the role of this latter state. Due to the low ligand field splitting, the filling of energy levels follows Hund's rule and forces the system into a high spin configuration.

In summary, from x-ray absorption spectroscopy measurements together with LDA and charge-transfer multiplet calculations, deeper insight into the electronic structure of $\text{LaFeAsO}_{1-x}\text{F}_x$ has been proposed. The O K edge is well described by LDA calculations. The influence of the Madelung

potential on different ions coincides in both experimental and theoretical spectra. The shift in the chemical potential is clearly visible in the absorption edge. Furthermore, a low Coulomb energy U significantly smaller than the conduction bandwidth can be expected.

Band effects have a significant influence also on the shape of the experimental Fe L -edge absorption spectra. A shift in the chemical potential toward higher energies is observed in agreement with the results of the O K edge, which stresses the existence of a moderate or low Hubbard U . Further valuable information could be extracted from Fe $L_{2,3}$ -edge absorption spectroscopy together with charge-transfer multiplet calculations in T_d symmetry. The extracted parameter set ap-

pears to be similar to what has been suggested from DFT calculations, especially the low crystal-field splitting¹⁸ and the small hopping parameters.¹⁹ Furthermore, due to small values of the charge-transfer energy Δ and the Hubbard U the system turns out to be very covalent similar to what has been predicted from DFT calculations.¹⁶ From the entirety of our results we conclude that LaFeAsO is a bandwidth-dominated material.

This investigation was supported by the DFG (Contracts No. SFB 463 and No. KR 3611/1-1) and DFG priority program (Contract No. SPP1133).

*Corresponding author. t.kroll@ifw-dresden.de

- ¹Y. Kamihara, T. Watanabe, M. Hirano, and H. Hosono, *J. Am. Chem. Soc.* **130**, 3296 (2008).
- ²H. Takahashi, K. Igawa, K. Arii, Y. Kamihara, M. Hirano, and H. Hosono, *Nature (London)* **453**, 376 (2008).
- ³H.-H. Wen, G. Mu, L. Fang, H. Yang, and X. Zhu, *Europhys. Lett.* **82**, 17009 (2008).
- ⁴Z.-A. Ren, J. Yang, W. Lu, W. Yi, G.-C. Che, X.-L. Dong, L.-L. Sun, and Z.-X. Zhao, *Mater. Res. Innovations* **12**, 105 (2008).
- ⁵X. H. Chen, T. Wu, G. Wu, R. H. Liu, H. Chen, and D. F. Fang, *Nature (London)* **453**, 761 (2008).
- ⁶H. Hunte, J. Jaroszynski, A. Gurevich, D. C. Larbalestier, R. Jin, A. S. Sefat, M. A. McGuire, B. C. Sales, D. K. Christen, and D. Mandrus, *Nature (London)* **453**, 903 (2008).
- ⁷C. Cao, P. J. Hirschfeld, and H.-P. Cheng, *Phys. Rev. B* **77**, 220506(R) (2008).
- ⁸H. Eschrig, arXiv:0804.0186v2 (unpublished).
- ⁹L. Shan, Y. Wang, X. Zhu, G. Mu, L. Fang, C. Ren, and H.-H. Wen, *Europhys. Lett.* **83**, 57004 (2008).
- ¹⁰G. Mu, X.-Y. Zhu, L. Fang, L. Shan, C. Ren, and H.-H. Wen, *Chin. Phys. Lett.* **25**, 2221 (2008).
- ¹¹I. I. Mazin, D. J. Singh, M. D. Johannes, and M. H. Du, *Phys. Rev. Lett.* **101**, 057003 (2008).
- ¹²K. Kuroki, S. Onari, R. Arita, H. Usui, Y. Tanaka, H. Kontani, and H. Aoki, *Phys. Rev. Lett.* **101**, 087004 (2008).
- ¹³L. Boeri, O. V. Dolgov, and A. A. Golubov, *Phys. Rev. Lett.* **101**, 026403 (2008).
- ¹⁴H.-J. Grafe *et al.*, *Phys. Rev. Lett.* **101**, 047003 (2008).
- ¹⁵T. Y. Chen, Z. Tesanovic, R. H. Liu, X. H. Chen, and C. L. Chien, *Nature (London)* **453**, 1224 (2008).
- ¹⁶D. J. Singh and M.-H. Du, *Phys. Rev. Lett.* **100**, 237003 (2008).
- ¹⁷K. Haule, J. H. Shim, and G. Kotliar, *Phys. Rev. Lett.* **100**, 226402 (2008).
- ¹⁸A. O. Shorikov, M. A. Korotin, S. V. Streltsov, S. L. Skornyakov, D. M. Korotin, and V. I. Anisimov, arXiv:0804.3283v2, *J. Theor. Exp. Phys.* (to be published).
- ¹⁹M. Daghofer, A. Moreo, J. Riera, E. Arrighoni, D. Scalapino, and E. Dagotto, arXiv:0805.0148v3 (unpublished).
- ²⁰E. Z. Kurmaev, R. Wilks, A. Moewes, N. Skorikov, Y. Izyumov, L. Finkelstein, R. Li, and X. Chen, arXiv:0805.0668, *Phys. Rev. B* (to be published).
- ²¹G. Giovannetti, S. Kumar, and J. van den Brink, *Physica B* **403**, 3653 (2008).
- ²²L. Craco, M. Laad, S. Leoni, and H. Rosner, *Phys. Rev. B* **78**, 134511 (2008).
- ²³S.-L. Drechsler, M. Grobosch, K. Koepernik, G. Behr, A. Koehler, J. Werner, A. Kondrat, N. Leps, C. Hess, R. Klingeler, R. Schuster, B. Büchner, and M. Knupfer, arXiv:0805.1321v1, *Phys. Rev. Lett.* (to be published).
- ²⁴H. H. Klauss *et al.*, *Phys. Rev. Lett.* **101**, 077005 (2008); H. Luetkens *et al.*, *ibid.* **101**, 097009 (2008); R. Klingeler, N. Leps, I. Hellmann, A. Popa, C. Hess, A. Kondrat, J. Hamann-Borrero, G. Behr, V. Kataev, and B. Büchner, arXiv:0808.0708v1 (unpublished); C. Hess, A. Kondrat, A. Narduzzo, J. E. Hamann-Borrero, R. Klingeler, J. Werner, G. Behr, and B. Büchner, arXiv:0811.1601 (unpublished).
- ²⁵The onset of the peaks has been defined as the photon energy at which the intensity reaches 10% of its value at the peak maximum.
- ²⁶A. Koitzsch, D. Inosov, J. Fink, M. Knupfer, H. Eschrig, S. Borisenko, G. Behr, A. Kohler, J. Werner, B. Büchner, R. Follath, and H. Durr, arXiv:0806.0833, *Phys. Rev. B* (to be published).
- ²⁷F. M. F. de Groot, *Coord. Chem. Rev.* **249**, 31 (2005).
- ²⁸L. Tröger, D. Arvanitis, K. Baberschke, H. Michaelis, U. Grimm, and E. Zschech, *Phys. Rev. B* **46**, 3283 (1992).
- ²⁹A. Koitzsch *et al.* (unpublished).
- ³⁰F. M. F. de Groot, J. C. Fuggle, B. T. Thole, and G. A. Sawatzky, *Phys. Rev. B* **42**, 5459 (1990).
- ³¹P. H. Butler, *Point Group Symmetry, Applications, Methods and Tables* (Plenum, New York, 1962).
- ³²R. D. Cowan, *The Theory of Atomic Structure and Spectra* (University of California Press, Berkeley, 1981).
- ³³B. T. Thole, G. van der Laan, J. C. Fuggle, G. A. Sawatzky, R. C. Karnatak, and J. M. Esteva, *Phys. Rev. B* **32**, 5107 (1985).